Dalton Transactions

Accepted Manuscript

ROYAL SOCIETY OF CHEMISTRY

www.rsc.org/dalton

Water-soluble Carboranyl-phthalocyanines for Boron Neutron Capture Therapy. Synthesis, Physico-chemical Properties, and in Vitro BNCT Tests of the Zn(II)-*nido*-carboranyl-hexylthiophthalocyanine

Daniela Pietrangeli,[a] Angela Rosa,[a] Antonietta Pepe,[a] Saverio Altieri,[b] Silva Bortolussi,[b] Ian Postuma,[b] Nicoletta Protti,[b] Cinzia Ferrari,[c] Laura Consolino,[c] Annamaria Clerici,[c] Elisa Viola,[d] Maria Pia Donzello,[d] and Giampaolo Ricciardi[*a]*

[a]*Dipartimento di Scienze, Università della Basilicata, Viale dell'Ateneo Lucano 10, 85100 Potenza, Italy. Fax: +39 0971 205678; Tel: +39 0971 205933; E-mail: giampaolo.ricciardi@unibas.it*

[b]*Dipartimento di Fisica, Università di Pavia e Istituto Nazionale di Fisica Nucleare (INFN), Sezione di Pavia, via Bassi 6, 27100 Pavia, Italy.*

[c]*Dipartimento di Scienze Clinico-Chirurgiche, Laboratorio di Chirurgia Sperimentale, Università di Pavia, Via Ferrata, 27100 Pavia, Italy.*

[d]*Dipartimento di Chimica, Università di Roma Sapienza, Piazzale A. Moro 5, I-00185 Roma, Italy.*

Abstract: The zinc(II) complex of the octa-anionic 2,3,9,10,16,17,23,24-octakis-(7-methyl-7,8-dicarba-*nido*-undeca-boran-8-*yl*)hexyl-thio-6,13,20,27-phthalocyanine (*nido*-[ZnMCHESPc]Cs_8, **7**) has been obtained in the form of caesium salt through mild deboronation of the neutral precursor, the *closo*-[ZnMCHESPc] complex, **6**, by CsF. **6** has been synthesized, in turn, by heating a finely ground mixture of the appropriate phthalonitrile and zinc(II) acetate at 180.0 ° C. The complexes have been characterized by elemental analyses, FT-IR, UV-visible absorption and fluorescence emission spectra, and their structure assessed by ^{1}H, ^{13}C, ^{11}B, and two-dimensional homo- and hetero-correlated NMR spectroscopy experiments. **7** showed appreciable solubility in water

solution, together with a marked tendency to aggregate. Aggregation of **7** in the hydrotropic medium resulted in a significant fluorescence quenching. Instead, fluorescence quantum yields (Φ_F) of 0.14 and 0.06, and singlet oxygen quantum yields (Φ_Δ) of 0.63 and 0.24 were obtained for **6** and **7**, respectively, in DMF solution. *In vitro* boron neutron capture therapy (BNCT) experiments, employing boron imaging techniques as implemented in qualitative and quantitative neutron autoradiography methods, showed that **7** is capable of increasing the boron concentration of two selected cancerous cell lines, the DHD/K12/TRb of rat colon adenocarcinoma and UMR-106 of murine osteosarcoma, with the large-size Cs^+ counter-ions used to neutralize the negatively charged carborane polyhedra not representing a significant obstacle to the process. Taken together, BNCT and photophysical results indicated that **7** is potentially suitable for bimodal or multimodal anticancer therapy.

Introduction

There is no doubt that liposomes of appropriate lipid formulation may represent, among others, effective intracellular delivery vehicles of carboranyl-tetrapyrroles for boron neutron capture therapy (BNCT) of cancer.[1-11] Generally, liposomes possess low toxicity and a remarkable ability to encapsulate and transport boron-rich solute molecules, including carboranyl-tetrapyrroles. Moreover these vesicles possess a sufficiently small size (30-150 nm) that enables them to pass through the porous immature vasculature of rapidly growing tumor tissue, hence conferring a certain degree of tumor specificity *via* the so called Enhanced Permeability and Retention (EPR) effect.[12] On their side, carboranyl-porphyrinoids, when loaded into liposomal carriers often retain the peculiar optical and photophysical properties of the macrocycle, that makes them suited not only for BNCT but also for complementary therapies, such photodynamic therapy (PDT) or photothermal therapy (PTT), depending on the nature of the macrocycle and/or of the coordinated metal.[6, 8, 13, 14] In spite of these remarkable advantages, the use of liposome as carriers of carboranyl-tetrapyrroles has the obvious implication that extrinsic, and not always innocuous synthetic compounds, are incorporated by the treated tissues, and a *direct* intracellular insertion of carboranyl-tetrapyrroles would be a biologically cleaner procedure.

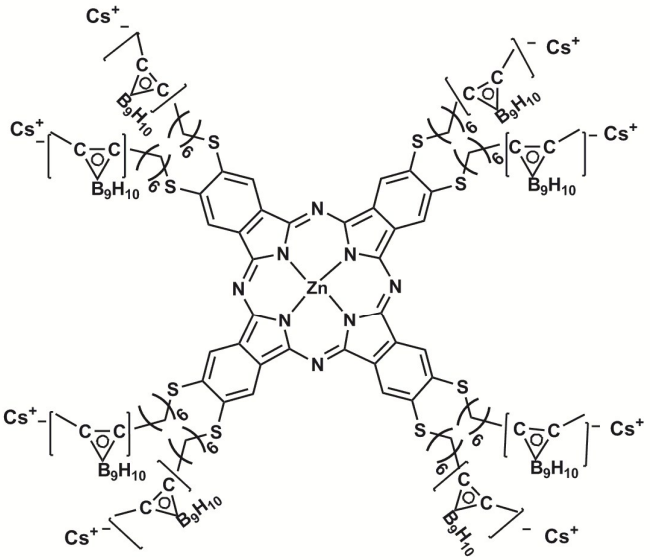

***nido*-[ZnMCHESPc]Cs_8**

As a matter of fact, a few water-soluble polyanionic or amphyphilic *nido*-carboranyl porphyrins have proven to effectively permeate the membrane of tumoral cells without the mediation of a carrier, and to retain both the whole boron content and the photophysical properties of the macrocyclic ring.[15-19] To the best of our knowledge there is only a report, instead, showing that polyanionic boron-containing phthalocyanines can be uptaken by cancerous cells.[20] This is most likely due to the paucity of sufficiently water-soluble phthalocyanines bearing highly boronated chemical functions.

To contribute to fill this gap, and in continuing our search for new molecules for application in boron neutron capture therapy (BNCT), we report herein the synthesis and the essential physical and chemical properties of the zinc(II) complex of the octa-anionic 2,3,9,10,16,17,23,24-octakis-(7-methyl-7,8-dicarba-*nido*-undeca-boran-8-*yl*)hexyl-thio-6,13,20,27-phthalocyanine, in the form of caesium salt (hereafter abbreviated *nido*-[ZnMCHESPc]Cs_8), and of the neutral precursor, the *closo*-[ZnMCHESPc] complex. It is shown, through qualitative and quantitative neutron autoradiography methods,[21, 22] that the polyanionic species is capable of increasing the boron concentration of two selected cell lines, the DHD/K12/TRb (DHD) of rat colon adenocarcinoma and UMR-106 (UMR) of murine osteosarcoma.

Experimental section

Materials: All chemicals and solvents (Aldrich Chemicals Ldt.) were of reagent grade and used in the syntheses as supplied. 1-methyl-*o*-carborane, purity <98%, was purchased from KATCHEM. Solvents used in the physical measurements were of spectroscopic or HPLC grade. THF was freshly distilled from sodium benzophenone ketyl under nitrogen.

Physical Measurements

(a) NMR spectroscopy. Two-dimensional (2D) NMR experiments were performed on a Varian Unity INOVA 500 MHz spectrometer equipped with a 5 mm triple-resonance probe and *z*-axial gradients. Two-dimensional Total Correlation Spectroscopy (*z*TOCSY) spectra were collected in the phase-sensitive mode using the States method. Typical data were 2048 complex data points, 32 or 64 transients and 256 increments. Relaxation delays were set to 1.5 s and spinlock (DIPSI3) mixing time was 80 ms. Shifted sine bell squared weighting and zero filling to 2K x 2K was applied before Fourier transform. Data were processed with VNMRJ 4.0. The 2D ^{1}H–^{13}C gradient Heteronuclear Single Quantum Correlation (adiabatic version) (gHSQCAD) and the gradient Heteronuclear Multi-Bond Connectivity (adiabatic version) (gHMBCAD) experiments were carried out using the pulse sequences from the Varian user library. The ^{13}C resonances were assigned through the 2D ^{1}H–^{13}C HSQC and ^{1}H–^{13}C HMBC spectra by using the assigned ^{1}H chemical shifts for proton resonances.

(b) Other physical measurements. IR spectra were measured with a FT/IR-460-Plus JASCO spectrometer. GC-MS spectra were measured with a Hewlett-Packard 6890. Elemental analyses were performed by the "Servizio di Microanalisi" at the Dipartimento di Chimica, Università "La Sapienza" (Rome) on an EA 1110 CHNS-O instrument. MALDI-ToF mass spectra were recorded

on a Ultrafelex III TOF-TOF instrument, Bruker Daltonics, using dihydroxybenzoic (DHB) acid 20 mg/mL in CH_3CN/TFA 0.1% 70/30 as the matrix. Data were acquired by Flex Control™ software.

Photophysical and photochemical measurements

(a) UV-visible spectra. UV-visible absorption spectra were recorded at room temperature on a Varian UV-Vis-NIR 05E Cary spectrophotometer.

(b) Fluorescence spectra. Steady-state fluorescence spectra were obtained with a Fluorescence Spectrophotometer (Cary Eclipse, Varian) using a 10 mm-quartz SUPRASIL cuvette. The fluorescence quantum yields were determined by a comparative method with a reference standard of chlorophyll-*a* (Φ_F = 0.32, ether solution), according to the equation

$$\Phi_F^S = \frac{G^S * n_{DMF}^2 * A^R}{G^R * n_{ether}^2 * A^S} \Phi_f^R$$

where *G* is the integrated emission area, *n* is the refractive index of the solvent, *A* is the absorbance at the excitation wavelength, *S* and *R* indicate the sample and the reference. In all cases the absorbance of the solution was below 0.1 at and above the excitation wavelength (λ_{exc} = 620 nm).

(b) Singlet oxygen quantum yield (Φ_Δ). The singlet oxygen quantum yield (Φ_Δ) of the investigated complexes was measured in DMF (ca. 10^{-6}-10^{-5} M in the complex) by an absolute method using 1,3-diphenylisobenzofuran (DPBF) as chemical quencher of $^1O_2$. For each experiment, the $1/\Phi_\Delta$ value was obtained as the intercept of a Stern-Volmer plot, according to the following equation:

$$\frac{1}{\Phi_{DPBF}} = \frac{1}{\Phi_\Delta} + \frac{k_d}{k_r}\frac{1}{\Phi_\Delta}\frac{1}{[DPBF]}$$

where k_d is the decay rate constant of $^1O_2$ in DMF, k_r is the rate constant of the quenching of $^1O_2$ by DPBF and Φ_{DPBF} is the quantum yield of the photoreaction.

The irradiation of the solution was carried out with a laser source (Premier LC Lasers/HG Lens, Global Laser) of appropriate wavelength - 685 nm (nominal), 680 (effective) - close to the Q-band maximum (698 nm) of the complexes, whose stability was also checked during irradiation. The laser emission power was accurately measured with a radiometer (ILT 1400A/SEL100/F/QNDS2, International Light Technologies) and usually adjusted to ca. 0.300 mW. A detailed description of the experimental procedure is illustrated in a recent publication.[8]

In vitro BNCT experiments. The formulations based on the *nido*-[ZnMCHESPc]Cs_8 salt were tested on two cell lines, already employed in BNCT research at University of Pavia (Italy): DHD/K12/TRb (DHD) of rat colon adenocarcinoma and UMR-106 (UMR) of murine osteosarcoma. The cells were treated following the same protocol used for boron uptake measurements and cell survival studies as a function of the absorbed dose. Cells were grown as confluent monolayer, at 37 °C humidified air, in a medium composed by a mixture (1:1) of HAM'S F10 and DMEM (Celbio), supplemented with 10% foetal bovine serum (Euroclone) and 40 μg/ml gentamicin. DMEM at low and high glucose concentration have been respectively used for DHD and UMR cells.

According to their different growing capability, the DHD line was seeded at the density of 3.0 x 10^6 cells in 75 cm^2 flasks, whereas the UMR at 1.5 x 10^6 cells/flask. After 48 h, cells were treated for 4h in medium enriched with *nido*-[ZnMCHESPc]Cs_8 at concentrations of 3 and 6 ppm in ^{10}B (natural isotopic abundance). At the end of the fixed contact time, the medium was removed and the cells washed three times with PBS, trypsinized, counted and splitted into two aliquots, one intended for the cytotoxicity test, the second for the analysis of the intracellular boron concentration. Control cells were processed in the same way as the *nido*-[ZnMCHESPc]Cs_8 treated samples.

For boron uptake measurements, cells were centrifuged (10′, 1200 rpm) to eliminate the medium with non-absorbed boron, and layered on mylar disks at the concentration of 4 x 10^6 cells/disk, where they had undergone a drying process before being measured. The two techniques used to

point out 10-B concentrations in cells are based on neutron autoradiography. This method is based on the employ of Solid State Nuclear Track Detectors (SSNTD), in particular policarbonate slides (CR-39). This material has the property to be insensitive to uncharged radiation as gamma rays or visible light, but it is sensitive to charged radiation. When a charged particle crosses the SSNTD it causes damage along its path, creating a latent track. This track can be enlarged and made visible under an optical microscope by a chemical etching properly optimized. Neutron autoradiography can be thus useful for studying the biodistribution of 10-B in samples deposited directly on the detector and irradiated in a thermal neutron field. The neutron capture in 10-B and in 14-N originates protons, alpha particles and lithium ions, that creates latent tracks in the CR-39, that can be visualized in order to investigate the presence of boron in the samples. The technique can be optimized to obtain two different kinds of results: the imaging of boron distribution, which is a qualitative result, and the quantitative measurement of its concentration. The first result is obtained by irradiating the samples in a position of the Thermal Column of the TRIGA reactor in Pavia, where the thermal neutron flux is about $2 \cdot 10^{9}$ n cm^{-2} s^{-1} at the maximum power of 250 kW. The irradiation time is 2 hours. This high fluence allows obtaining a distribution of tracks in CR-39 that is a map of boron distribution in the sample. The etching is then performed in a NaOH solution, 6.25 N, at 70°C for 20 min. The result is a neutron autoradiography of the sample, where the darker areas correspond to the zones of the sample with higher boron concentration. These images allow analyzing the homogeneity of boron distribution in the whole sample, and, in case of tissues, to visualize if boron is taken up preferentially by tumor cells by comparison with a contiguous tissue section stained for standard histology.[21] In the case of cell samples, it is useful to compare different administration protocols and to evidence if a boron carrier is effective for the type of cells under study. This method cannot be employed to quantify boron. To this end, it is necessary that the tracks are well separated and sufficiently large to be classified and counted using suitable software. The samples are thus irradiated in the same position, but at a reactor power of 1 kW for 30 minutes, receiving a thermal neutron fluence of about 10^{10} n cm^{-2}. The etching is then performed in a NaOH

solution 6.25 N at 70°C for 125 minutes. A previous calibration obtained with standard samples with known boron concentration[22] gives the relation between the superficial density of tracks and boron concentration. The two different applications allow, in case of not uniform boron distribution, measuring boron concentration separately for the different areas of the sample, but in case of cell samples, boron concentration is usually homogeneous.

Synthetic procedures

1-methyl-2-(1-bromohex-6-yl)-1.2-*closo*-dodecaborane (2). This compound was prepared according to a slightly modified literature procedure.[23] A solution of 1-methyl-1,2-dicarba-*closo*-dodecaborane, 1, (2.4 g, 15.2 mmol) in freshly distilled THF (20 mL) was cooled to –50 °C. A 1.3 M solution of n-BuLi in hexane (14 mL; 15.2 mmol + 20% excess) was added, under Ar, dropwise with stirring. The mixture was allowed to stir for 2 h while being warmed to ambient temperature. The solution was cooled to –78 °C and 1,6-dibromohexane (23.4 mL, 152 mmol) was added rapidly. The mixture was allowed to stir for 2 h while being warmed to ambient temperature. After quenching with water (15 mL), the mixture was transferred to a separatory funnel and diluted with $CHCl_3$ (10 mL). The layers were separated and the aqueous layer was extracted with additional $CHCl_3$ (2 x 15 mL). The organic layer was dried over anhydrous Na_2SO_4 and concentrated in vacuo to give a colorless oil. The crude product was distilled under vacuum to remove the excess of 1,6-dibromohexane and then purified by chromatography on silica-gel (pentane/$CHCl_3$ 95:5, R_f = 0.43) to give a colorless oil. Yield: 90% (4.2 g, 13.1 mmol). ^{1}H NMR δ_H(500 MHz, $CDCl_3$, Me_4Si) 3.43 (2H, t, *J*= 7Hz, CH_2Br), 2.18 (2H, m), 2.02 (3H, s, Cc-CH3), 1.88 (2H, qt, *J*= 7 Hz), 1.59 (2H, m(qt)), 1.49 (2H, m(qt)), 1.36 (2H, m(qt), B-H), 2.8-1.4 (10H, m). ^{13}C NMR δ_C (125 MHz, $CDCl_3$, Me_4Si) 78.3, 79.4, 35.4, 33.9, 32.7, 29.7, 28.6, 27.9, 23.4. ^{11}B NMR δ_B (128 MHz, $CDCl_3$, $BF_3{\cdot}OEt_2$) –4.3 (1B), –5.6 (1B), –9.0 (2B), –9.7 (2B), –12.5 (4B). MS (EI) *m/z* calcd for $[C_9H_{29}B_{10}Br]^+$: 321.3; found 321.

1-methyl-2-(1-thioacetylhex-6-yl)-1,2-*closo*-dodecaborane (3). To a solution of **2** (3.54 g, 5.1 mmol) in an EtOH/THF 2:1 mixture (30 mL), AcSK (1.51 mg, 13.2 mmol) was added. The mixture was allowed to stir for 4 h at room temperature, and then concentrated in vacuo. The crude product was diluted with $CHCl_3$ (15 mL) and the organic layer was washed with distilled water (3 x 20 mL), dried over anhydrous Na_2SO_4 and concentrated in vacuum. The product was purified by chromatography on silica-gel (pentane/CH_2Cl_2, 7:3) to give a white solid. Yield: 95% (3.4 g, 10.6 mmol). ^{1}H NMR δ_H(400 MHz, $CDCl_3$, Me_4Si) 2.75 (2H, t, *J*= 7 Hz, -C*H*$_2$-S-), 2.22 (3H, s, C_{carb}-C*H*$_3$), 2.05 (2H, m), 1.9 (3H, s, CH_3-C=O), 1.45 (4H, m), 1.25 (4H, m), 2.9-1.5 (80H, br, B-*H*). ^{13}C NMR δ_C (100 MHz, $CDCl_3$, Me_4Si) 196.0, 78.4, 74.9, 35.5, 30.9, 29.7, 29.6, 29.1, 28.9, 28.5, 23.3.

1-methyl-2-(1-thiohex-6-yl)-1,2-*closo*-dodecaborane (4). To a solution of **3** (3.4 g, 10.6 mmol) in MeOH (120 mL) concentrated HCl (35%, 12 mL) was added. The mixture was allowed to stir for 3 h at room temperature and then concentrated in vacuo. The crude product was diluted with CH_2Cl_2 (50 mL) and the organic layer was washed with distilled water (3 x 30 mL), dried over anhydrous Na_2SO_4 and concentrated in vacuum. The product was used without further purification. MS (EI) *m/z* calcd for $[C_9H_{24}B_{10}S]^+$: 274.4; found: 274.

4,5-dithiohexyl(1-methyl-1,2-*closo*-dodecaboran-2yl)-1,2-dicyanobenzene (5). According to a procedure reported by some of us,[24] 4,5-dichloro-1,2-dicyanobenzene (355 mg, 1.8 mmoL) and **4** (2.9 g, 10.6 mmol) were dissolved in dry DMSO (20 mL). The solution was warmed to 45 °C and anhydrous K_2CO_3 (3 g, 22 mmol) was added in small portions over 1 h. The reaction mixture was stirred at 45 °C for 3 h. The solution was cooled and then diluted with CH_2Cl_2. The organic layer was washed with distilled water (4 x 20 mL), dried over anhydrous Na_2SO_4 and concentrated in vacuo. The crude product was purified by chromatography on silica-gel (CH_2Cl_2/hexane 7:3). Yield: > 95% (1.22 g, 1.8 mmol). Melting point: 174 °C (uncorrected). ^{13}C NMR δ_C (100MHz,

$CDCl_3$, Me_4Si) 144.2, 128.4, 115.8, 111.5, 78.1, 74.8, 35.4, 32.8, 29.6, 28.9, 28.6, 28.1, 23.4. ^{11}B NMR δ_B (128 MHz, $CDCl_3$, $BF_3{\cdot}OEt_2$): – 4.31 (1B), – 5.57 (1B), – 9.10 (2B); –9.64 (2B), –10.49 (4B). FT-IR (KBr disk) cm^{-1}: 3079; 2935; 2859; 2584 (ν_{B-H}); 2230; 1538; 1456; 1109; 731; 526. HRMS ESI-MS *m/z* for $[C_{26}H_{52}B_{20}N_2S_2+Br]^-$: 752.5335; found: 752.4754. Elemental analyses (%) for $C_{26}H_{52}B_{20}N_2S_2$: C 46.40, H 7.79, N 4.16, S 9.53; found C 45.66, H 7.52, N 3.98, S 9.78.

[2,3,9,10,16,17,23,24-octakis-(1-methyl-1,2-*closo*-dodecaboran-8-yl)hexylthio-6,13,20,27-phthalocyaninato zinc(II)] (6). **5** (267 mg, 0.40 mmol) and Zn(acetate)·H_2O (33 mg, 0.15 mmol) were finely grounded and heated at 180°C under N_2 for 15h. The cooled dark-green powder was extracted with $CHCl_3$, concentrated in vacuum, and repeatedly (5 times) recrystallized from CH_2Cl_2/MeOH (1:1, v:v). To remove the residual (yellowish) impurities, the product was passed on neutral alumina using, in sequence, a CH_2Cl_2/MeOH (7:3, v:v) mixture and CH_2Cl_2/Hexane (9:1, v:v) as eluents. The resulting dark-green microcrystalline product was air dried at 50 °C for 3 h. Yield: 31% (85 mg, 0.031 mmol). MALDI-ToF *m/z* for $[C_{104}H_{208}B_{80}N_8S_8Zn]^+$: 2757.616; found: 2757.422. Elemental analyses calcd (%) for $C_{104}H_{208}B_{80}N_8S_8Zn{\bullet}C_6H_{14}$: C 46.46, H 7.87, N 3.94; found: C 46.49; H, 7.41; N 2.37.

[2,3,9,10,16,17,23,24-octakis-(7-methyl-7,8-dicarba-*nido*-undecaboran-8-yl)hexylthio-6,13, 20,27-phthalocyaninato zinc(II)]Cs_8 (7). To a solution of **6** (78 mg, 0.028 mmol) in THF (7 mL) a solution of CsF (138 mg, 0.91 mmol) in EtOH (14 mL) was added. The mixture was stirred at 80°C for 48 h. The solution was cooled, concentrated in vacuum, and the resulting dark-green solid was passed on a Dowex resin in the Cs^+ form using water as eluent. FT-IR (film on KBr disk, cm^{-1}) 3316, 2931, 2856, 2516 (ν_{B-H}), 1598. Elemental analyses calcd (%) for $C_{104}H_{208}B_{72}N_8S_8Cs_8Zn$: C 33.45, H 5.61, N 3.00, S 6.87 ; found: C 32.95, H 5.54, N 2.32, S 7.09.

Results and discussion

Synthesis and characterization. As displayed in Scheme 1, the *nido*-[ZnMCHESPc]Cs_8 salt, **7**, could be synthesized by effective (>60%) conversion of the *closo*-[ZnMCHESPc] complex, **6**, in the nido form upon treatment with CsF in a EtOH/THF mixture. In turn, the neutral precursor **6** was obtained in more than acceptable yield (31%) by heating a finely ground mixture of the phthalonitrile **5** – resulting from a quantitative base-catalyzed aromatic nucleophilic substitution of **4** on 4,5-dichloro-1,2-dicyanobenzene – and zinc(II) acetate at 180.0 ° C for 2–4 hours.

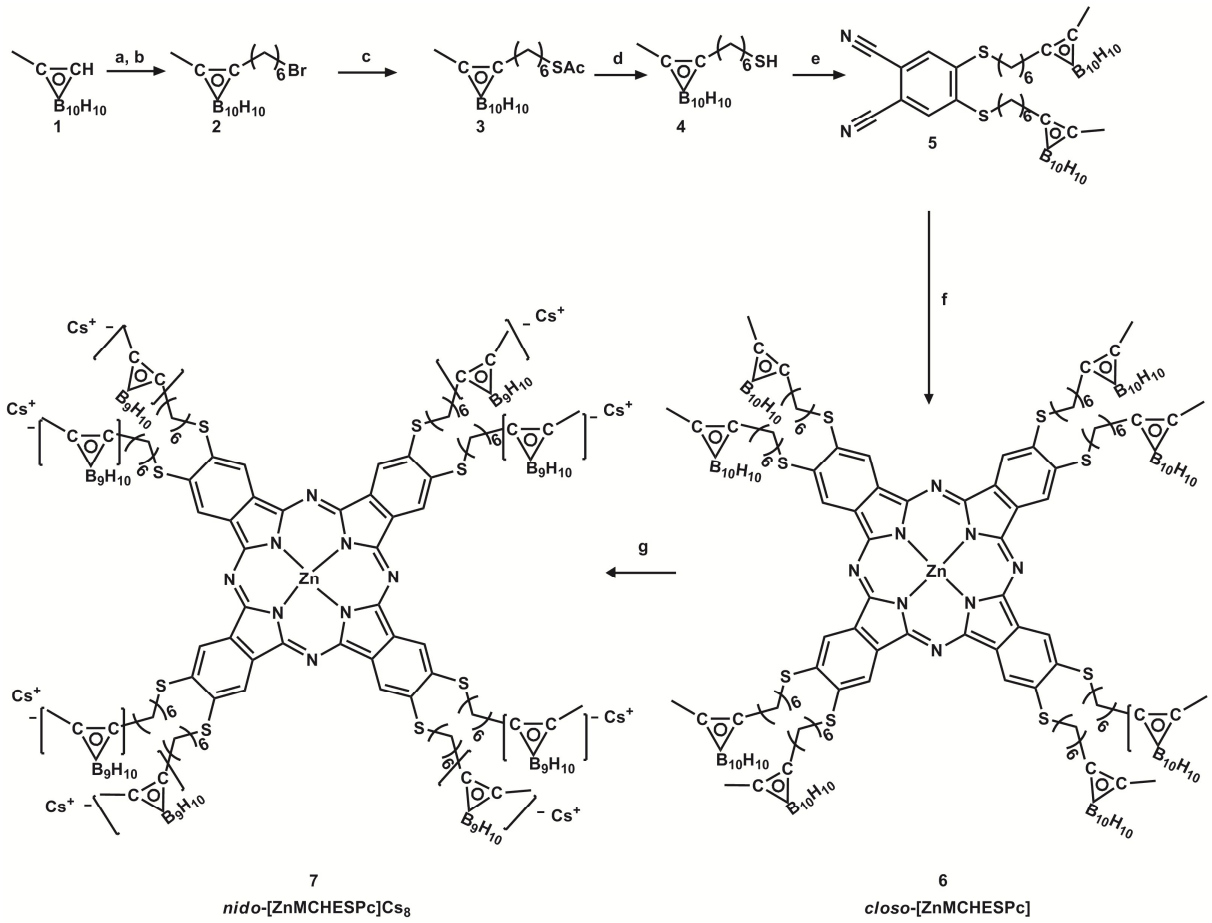

Scheme 1. Synthetic pathway to the neutral *closo*-[ZnMCHESPc] complex and the polyanionic derivative *nido*-[ZnMCHESPc]Cs_8. Reagents and conditions: (a) *n*-BuLi, THF, Ar, – 50 °C - r. t., 2h; (b) 1,6 - dibromohexane, – 78 °C - r. t., 2 h; (c) AcSK, EtOH/THF 2:1, r. t., 4 h; (d) HCl_{aq}

(35%), MeOH, r. t., 3h; (e) 4,5-dichloro - 1,2 - dicyanobenzene, K_2CO_3, DMSO, 45 °C, 3 h; (e) $Zn(acetate)_2 \cdot H_2O$, 180 °C, 15h; (f) DOWEX resin in the Cs^+ form.

Special care was paid to the purification of **6** from the persistent by-products. To this end the complex was recrystallized at least 5 times from CH_2Cl_2/MeOH mixtures and, subsequently, passed on neutral alumina using, in sequence, a CH_2Cl_2/MeOH (7:3, v:v) and a CH_2Cl_2/hexane (9:1, v:v) mixture as eluents. Satisfactory analytical data were obtained for **6** and **7**.

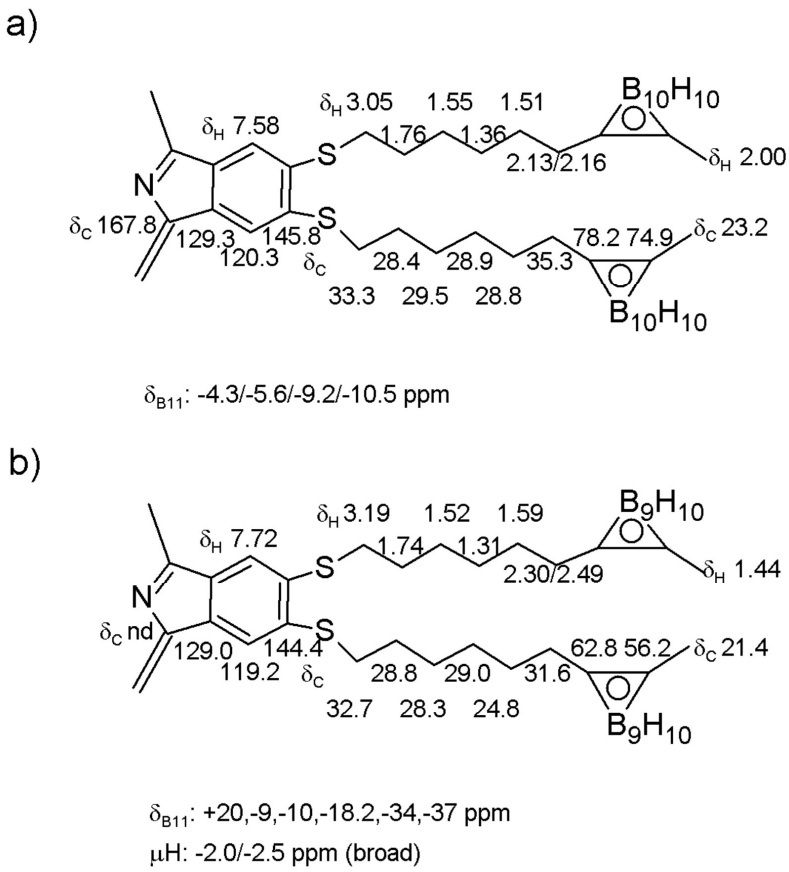

Fig. 1. Schematic representation of the symmetry-equivalent fragments constituting the molecular structure of the *closo*-[ZnMCHESPc] (a) and *nido*-[ZnMCHESPc]Cs_8 (b) complex with the indication of the ^1H and ^{13}C chemical shifts recorded at 298 K in $CDCl_3$ and acetone-d_6, respectively; the ^{11}B chemical shifts of the boron atoms belonging to the *o*-carborane moieties in the neutral complex, and the ^{11}B and μH chemical shifts of the pertinent atoms belonging to the *nido*-carborane moieties of the *nido*-[ZnMCHESPc]Cs_8 complex are also indicated.

Dissimilar from the neutral parent **6**, but similar to other polyanionic carboranyl-Pcs, **7** proved to be silent at a MALDI-ToF mass spectral analysis.[1, 24]

A complete ^{1}H, ^{13}C and ^{11}B NMR spectral characterization of both, the neutral *closo*-[ZnMCHESPc] and the octaanionic *nido*-[ZnMCHESPc]Cs_8 complexes, was accomplished by two-dimensional homo- and hetero-correlated spectroscopy experiments in $CDCl_3$ and acetone-d_6, respectively. The resulting spectral data are displayed in Fig. 1.

In the δ 1.20-3.50 ppm spectral region of the ^{1}H spectra the signals of the hexylthio-chain protons highly overlapped with those of the carborane protons. Two broad signals at δ –2.00 and –2.50 ppm were observed in the ^{1}H spectrum of the nido complex, corresponding to the *endo* protons of the anionic carborane polyhedra.

The aromatic protons belonging to the phthalocyanine core showed resonances at δ 7.58 and 7.62 ppm for the closo and nido compound, respectively. The complete ^{1}H chemical shift assignments of the hexylthio chain protons were achieved by TOCSY experiments, connecting all protons in the scalar coupled spin system of the hexylthio chain, while the ^{13}C chemical shifts of the corresponding carbons were assigned by the hetero-correlated single-bond HSQC experiments, correlating protons with directly attached carbons. Finally, the assignment of the aromatic carbons of the phtalocyanine moiety was accomplished through long-range hetero-correlated HMBC experiments. The ^{11}B chemical shifts observed for the closo and the nido compounds were in accordance with those expected for the two different carboranyl structures.

Both the neutral and the polyanionic form of the investigated Pcs resulted to be chemically stable in DMF, where they are highly soluble and exhibit the typical electronic absorption spectra of monomeric Pcs, with strong Q(0,0) bands at 696 nm. The *nido*-[ZnMCHESPc]Cs_8 complex showed appreciable solubility and remarkable chemical stability in water. The electronic spectrum of this compound in water showed, however, even at very low concentrations (< 10^{-6} M), a 50 nm blue

shift of the Q(0,0) absorption relative to the mononuclear species, and broadening, which are spectral signatures of co-facial aggregation of the Pc ring.[25, 26]

Aggregation could be gradually disrupted by progressive addition of DMF, however. In a totally reversible way, addition of water to DMF solutions of **7** resulted in the aggregation of the complex. As inferred from Fig. 2, where the Q band region of the absorption spectrum of *nido*-[ZnMCHESPc]Cs_8 in a series of DMF-water mixtures is shown, on increasing the water proportion the intensity of the Q band of the monomer (696 nm) decreases with a concomitant increase of the band at 646 nm, and at least three isosbestic points, at 427, 673, and 730 nm are observed.

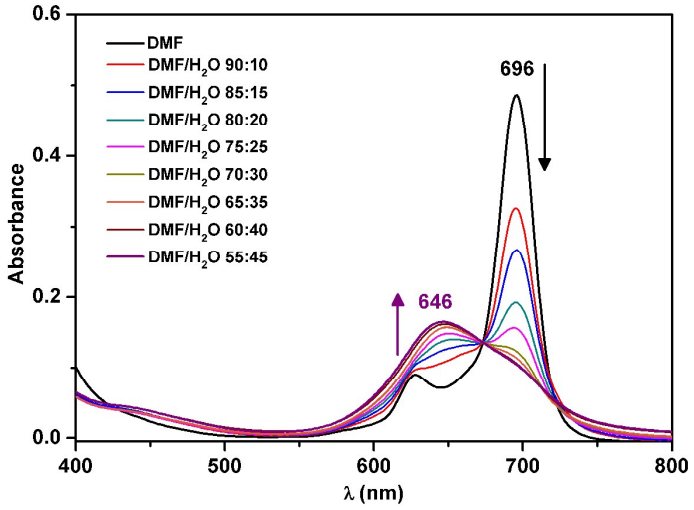

Fig. 2. Electronic absorption spectrum of *nido*-[ZnMCHESPc]Cs_8 in water-DMF mixtures with increasing water proportion.

Overall, this behavior is indicative a monomer-dimer equilibrium, and is strongly reminiscent of that shown in water/methanol solutions by a number of tetra-cationic Pcs bearing quaternized pyridinium functions.[27] Just as observed in the case of these tetra-cationic Pcs, the dimeric form, which dominates in the hydrotropic medium, is not emissive, while the monomeric form characterizing the DMF solution is fluorescent.[27] For this reason, photoactivity of both complexes **6** and **7** was investigated in DMF solution, and their fluorescence (Φ_F) and singlet oxygen (Φ_Δ) quantum yields were measured, as reported in Table 1. The fluorescence quantum yield determined

for **7** in DMF was smaller than that measured for the neutral counterpart **6** (0.06 vs 0.14, see Table 1), most likely because of intermolecular (external) heavy-atom effects.[28]

Table 1. Photophysical and photochemical properties of the *closo*-[ZnMCHESPc] and *nido*-[ZnMCHESPc]Cs_8 complexes in DMF solution.

	Singlet oxygen			Fluorescence		
	λ_{max}(nm)	λ_{irr} (nm)	Φ_Δ [a]	λ_{exc}(nm)	λ_{em} ($\Delta\lambda$) [b] (nm)	Φ_F [a]
closo-[ZnMCHESPc]	696	680	0.63	620	710 (14)	0.14
nido-[ZnMCHESPc]Cs_8	696	680	0.24	620	714 (18)	0.08

[a]Mean value of at least three measurements. Uncertainty is half dispersion and it is typically ± 0.03. [b]$\Delta\lambda$ is the Stokes shift.

The singlet oxygen quantum yield measured for **7** was relatively low (0.24), most likely due to a combination of events, namely, (i) fast recovery of the ground-state upon heavy atom induced efficient T_1/S_0 Intersystem Crossing (ISC) and (ii) scarce capability of the nido-carboranyl cages to protect the phthalocyanine against intermolecular quenching (*vide infra*). It is reasonable to assume that replacing the Cs^+ counter-ions by lighter alkaline metal ions, such as Na^+ or K^+, would improve the singlet oxygen quantum yield. Nevertheless, the singlet oxygen quantum yield measured for **7** is sufficiently high for this complex to be used in complementary PDT therapy, provided that an effective dimerization control in the biological fluids is set up. However, the possible dimerization of the complex in biological environment should not be regarded, in principle, as a totally negative feature. In fact, the dimer, after photo-excitation into the still intense Q-band is expected to undergo (fast) ground state recovery, and to release thermal energy, that would make the complex suitable for PTT complementary therapy. It is useful to remind, in this respect, that the normally emissive Pd(II) and Pt(II) octabutoxynaphthalocyanines, upon intracellular localization in the form of aggregated clusters and subsequent irradiation, are able to cause an extensive cell death, with the photoinduced cell damage being typical of photothermal sensitisation processes.[29]

Worth mentioning, the neutral complex **6** showed a remarkably high (0.63) singlet oxygen quantum yield, that is significantly larger than that of ZnPc (0.53)[30] and 2,9,16,23-tetrasulfophthalocyanine

zinc(II) (ZnPTS) (0.45),[30] and compares well with that measured by Jori and coworkers for a tetra-carboranyl-methylphenoxy-substituted Zn(II) phthalocyanine (0.67)[6] and by Wohrle and coworkers for the best performing member of a series of *o*-carboranyl substituted ZnPcs (0.65).[30] What we find indicates that **6** is a prominent sensitizer for PDT, and confirms the suggestion by Wohrle and coworkers according to that the carboranyl substituents partially protect the phthalocyanine against intermolecular quenching.[30]

To evaluate the potential of the polyanionic complex **7** in BNCT, the molecule was tested on two cell lines, already employed in BNCT research at the University of Pavia, namely DHD/K12/TRb (DHD) of rat colon adenocarcinoma and UMR-106 (UMR) of murine osteosarcoma. Before performing BNCT experiments, the *nido*-[ZnMCHESPc]Cs_8 cytotoxicity was evaluated by means of the plating efficiency test. Briefly, treated and control cells were plated at three different concentrations (50, 100, 250 cells/Petri) in five replicate Petri dishes for each of them and allowed to grow at 37 °C for about 10 days. Subsequently, the colonies were fixed, stained, and counted for the estimation of the fraction of cells surviving after the treatment. The obtained surviving cell percentage following treatment with **7** for 4h at different ^{10}B concentrations (3 ppm and 6 ppm, 10-B natural abundance) administered to cell cultures indicated that no significant toxic effects were noticed on UMR cells, while a moderate concentration-dependent cytotoxicity was observed on DHD cells line (98% and 84% was the fraction of cells surviving after the 3 and 6 ppm ^{10}B treatment, respectively). In conducting in vitro BNCT experiments, the investigated cell lines were seeded at a different density, according to their different growing capability. Namely, the DHD line was seeded at the density of 3.0×10^6 cells/flask, whereas the UMR line was seeded at 1.5×10^6 cells/flask. After 48 h, both cell lines were treated for 4h in a medium containing **7** at concentrations of 3 and 6 ppm. Table 3 lists the results obtained by quantitative neutron autoradiography of DHD and UMR cell samples treated with the **7** at different ^{10}B (natural abundance) concentrations. For each protocol at least three samples were tested. The error associated with the measurements is connected to the count of tracks in the various pictures taken from each sample. The standard

deviation of the results obtained in the different samples treated with the same protocol is considerably lower than this error.

Table 2. ^{10}B concentration (in ppm) in the cell samples treated with **7** at two different initial concentrations, for 4 hours.

Protocol	Boron concentration in ppm (µg of 10-B per g of cells)
UMR (control)	0.6± 0.4
UMR + **7** (3 ppm)	1.9± 0.7
UMR + **7** (6 ppm)	3.2± 0.5
DHD (control)	1.4± 0.6
DHD + **7** (3 ppm)	2.7± 1.1
DHD + **7** (6 ppm)	3.1± 1.0

Boron imaging was performed in these samples. Being the absolute boron concentration not very high, not all the images are easy to interpret if compared with the controls. But in case of the samples treated with 6 ppm of 10-boron, it is possible to visualize the higher boron concentration, as seen by comparing the obtained neutron autoradiography image with the control one (Fig. 3).

Fig. 3. Imaging by neutron autoradiography of UMR control cells, not treated with boron (left) and UMR cells treated with an amount of **7** containing 6 ppm of 10-boron (natural abundance) for 4 hours (right).

Conclusions

In summary, two highly boronated phthalocyanines, the neutral *closo*-[ZnMCHESPc] complex and the polyanionic *nido*-[ZnMCHESPc]Cs_8 complex, have been synthesized and their physico-chemical properties in solution analyzed in some detail. It has been shown, through qualitative and quantitative neutron autoradiography methods, that *nido*-[ZnMCHESPc]Cs_8 complex is capable of creating higher boron concentrations in two selected cancerous cell lines, the DHD/K12/TRb of rat colon adenocarcinoma and UMR-106 of murine osteosarcoma, with the presence of counter-ions as large as the Cs^+ ions do not representing a significant obstacle to the process.

In consideration of the *in vitro* BNCT results and the photophysical and photochemical data, the *nido*-[ZnMCHESPc]Cs_8 complex has good potentialities for applications in bimodal and even multimodal anticancer therapies.

Worth noting, the parent neutral complex thanks to the remarkably high singlet oxygen quantum yield and the high boron content may also find application in combined PDT and BNCT anticancer therapies, provided that an appropriate intracellular delivery agent is used for this species.

Acknowledgements. The research was in part financially supported by Università della Basilicata (RIL-2011 Funds) and by Basilicata Innovazione. DP and GR thank Università di Roma "La Sapienza," Italy, and Dr. A. Vassallo, Università della Basilicata, Potenza, Italy, for performing microanalyses and mass spectra, respectively. GR thanks Claudio Barlabà for the valuable technical support.

References

1. D. Pietrangeli, A. Rosa, S. Ristori, A. Salvati, S. Altieri and G. Ricciardi, *Coord. Chem. Rev.*, 2013, 257, 2213-2231.
2. D. Samaroo, E. Perez, A. Aggarwal, A. Wills and N. O'Connor, *Ther. Deliv.*, 2014, 5, 859-872.
3. S. Ristori, A. Salvati, G. Martini, O. Spalla, D. Pietrangeli, A. Rosa and G. Ricciardi, *J. Am. Chem. Soc.*, 2007, 129, 2728-2729.
4. A. Salvati, S. Ristori, J. Oberdisse, O. Spalla, G. Ricciardi, D. Pietrangeli, M. Giustini and G. Martini, *J. Phys. Chem. B*, 2007, 111, 10357-10364.
5. A. Salvati, S. Ristori, D. Pietrangeli, J. Oberdisse, L. Calamai, G. Martini and G. Ricciardi, *Biophys. Chem.*, 2007, 131, 43-51.
6. E. Friso, G. Roncucci, D. Dei, M. Soncin, C. Fabris, G. Chiti, P. Colautti, J. Esposito, L. De Nardo, C. R. Rossi, D. Nitti, F. Giuntini, L. Borsetto and G. Jori, *Photochem. Photobiol. Sci.*, 2006, 5, 39-50.
7. D. Awad, I. Tabod, S. Lutz, H. Wessolowski and D. Gabel, *J. Organomet. Chem.*, 2005, 690, 2372-2375.
8. M. P. Donzello, E. Viola, M. Giustini, C. Ercolani and F. Monacelli, *Dalton Trans.*, 2012, 41, 6112-6121.
9. M. F. Hawthorne and K. Shelly, *J. Neurooncol.*, 1997, 33, 53-58.
10. E. M. Heber, M. F. Hawthorne, P. J. Kueffer, M. A. Garabalino, S. I. Thorp, E. C. C. Pozzi, A. M. Hughes, C. A. Maitz, S. S. Jalisatgi, D. W. Nigg, P. Curotto, V. A. Trivillin and A. E. Schwint, *Proc. Natl. Acad. Sci. U.S.A.*, 2014, 111, 16077-16081.
11. S. Tachikawa, T. Miyoshi, H. Koganei, M. E. El-Zaria, C. Vinas, M. Suzuki, K. Ono and H. Nakamura, *Chem. Commun.*, 2014, 50, 12325-12328.
12. A. Salvati, A. S. Pitek, M. P. Monopoli, K. Prapainop, F. Baldelli Bombelli, P. M. Kelly, C. Aberg, E. Mahon and K. A. Dawson, *Nature Nanotech.*, 2013, 8, 137.
13. S. Altieri, M. Balzi, S. Bortolussi, P. Bruschi, L. Ciani, A. M. Clerici, P. Faraoni, C. Ferrari, M. A. Gadan, L. Panza, D. Pietrangeli, G. Ricciardi and S. Ristori, *J. Med. Chem.*, 2009, 52, 7829-7835.
14. M. Hoebeke, *J. Photochem. Photobiol. B: Biol.*, 1995, 28.
15. M. G. H. Vicente, D. J. Nurco, S. J. Shetty and et al., *J. Photochem. Photobiol. B: Biol.*, 2002, 68, 123-132.

16. M. G. H. Vicente, B. F. Edwards, S. J. Shetty, Y. Houb and E. B. James, *Bioorg. Med. Chem.*, 2002, 10, 481-492.
17. M. G. H. Vicente, A. Wickramasinghe, D. J. Nurco, H. J. H. Wang, M. M. Nawrocky, M. S. Makarc and M. Miurac, *Bioorg. Med. Chem.*, 2003, 11, 3101-3108.
18. S. Kawabata, W. Yang, R. F. Barth, W. Gomg, T. Huo, P. J. Binns, K. J. Riley, O. Ongayi, W. Gottumukkala and M. G. H. Vicente, *J. Neurooncol.*, 2011, 103, 175-185.
19. V. A. Ol'shevskaya, R. G. Nikitina, A. V. Zaitsev, V. N. Luzgina, E. G. Kononova, T. G. Morozova, V. V. Drozhzhina, O. G. Ivanov, M. A. Kaplan, V. N. Kalinin and A. A. Shtil, *Org. Biomol. Chem.*, 2006, 4, 3815-3821.
20. A. V. Shmal'ko, A. V. Efremenko, A. A. Ignatova, I. B. Sivaev, A. V. Feofanov, E. Hamuryudan, A. Gül, L. V. Kovalenko, S. Qi and V. I. Bregadze, *J. Porphyrins Phthalocyanines*, 2014, 18, 960-966.
21. S. Altieri, S. Bortolussi, P. Bruschi, P. Chiari, F. Fossati, S. Stella, U. Prati, L. Roveda, A. Zonta, C. Zonta, C. Ferrari, A. Clerici, R. Nano and T. Pinelli, *Appl. Radiat. Isot.*, 2008, 66, 1850-1855.
22. M. A. Gadan, S. Bortolussi, I. Postuma, F. Ballarini, P. Bruschi, N. Protti, D. Santoro, S. Stella, L. Cansolino, A. Clerici, C. Ferrari, A. Zonta, C. Zonta and S. Altieri, *Nucl. Instrum. Meth. B.*, 2012, 51-56.
23. L. Ma, F. Hamdi, F. Wong and M. F. Hawthorne, *Inorg. Chem.*, 2006, 45, 278-285.
24. D. Pietrangeli, A. Rosa, A. Pepe and G. Ricciardi, *Inorg. Chem.*, 2011, 50, 4680-4682.
25. P. C. Martin, M. Gouterman, B. V. Pepich, G. E. Renzoni and D. C. Schindele, *Inorg. Chem.*, 1991, 30, 3305-3309.
26. E. S. Dodsworth, A. B. P. Lever, P. Seymour and C. C. Leznoff, *J. Phys. Chem.*, 1985, 89, 5698-5705.
27. T. Teixeira Tasso, Y. Yamasaki, T. Furuyama and N. Kobayashi, *Dalton Trans.*, 2014, 43, 5886-5892.
28. M. Rae, F. Perez-Balderas, C. Baleizão, A. Fedorov, J. A. S. Cavaleiro, A. C. Tomé and M. N. Berberan-Santos, *J. Phys. Chem. B*, 2006, 110, 12809-12814.
29. M. Camerin, S. Rello-Varona, A. Villanueva, M. A. Rodgers and G. Jori, *Lasers Surg. Med.*, 2009, 41, 665-673.
30. D. Wöhrle, O. Tsaryova, A. Semioshkin, D. Gabel and O. Suvorova, *J. Organomet. Chem.*, 2013, 747, 98-105.

Graphic Content

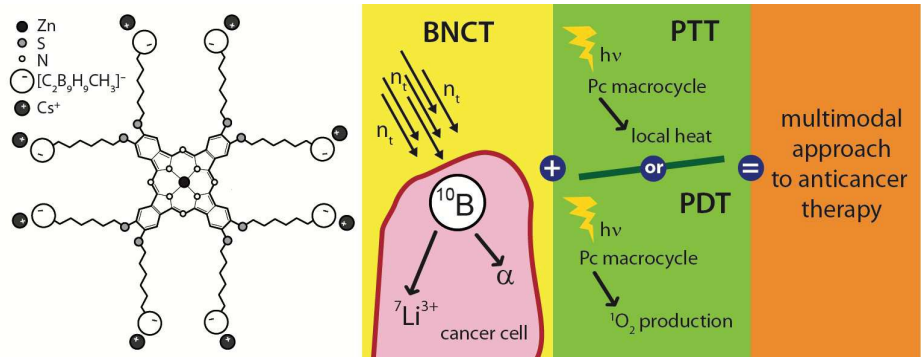

Synopsis

The *nido*-[ZnMCHESPc]Cs_8 complex is capable of increasing the boron concentration in the DHD/K12/TRb rat colon adenocarcinoma and UMR-106 of murine osteosarcoma cells.